Investigating structural changes and surface modification in glassy carbon induced by xenon ion implantation and heat treatment

M. Y. A. Ismail[1,2,*], Z. A. Y. Abdalla[1], E. G. Njoroge[1,3], O. S. Odutemowo[1], J. B. Malherbe[1], T. T. Hlatshwayo[1], E. Wendler[4], J. Aftab[2], H. Younis[2]

[1]*Department of Physics, University of Pretoria, Pretoria, 0002 South Africa*

[2]*Department of Physics, COMSATS University Islamabad, Islamabad, 45550 Pakistan*

[3]*ENGAGE, University of Pretoria, Pretoria, Pretoria, 0002 South Africa*

[4]*Institut für Festkörperphysik, Friedrich-Schiller Universität, 07743 Jena, Germany*

Highlights

- Implantation at room temperature led to amorphisation of glassy carbon structure.
- Highly recovery of the damaged region was observed after annealing at 1500 °C.
- The HRTEM of the virgin glassy carbon exhibited some features similar to fullerenes.
- The onion-like features suggest that glassy carbon is a disordered form of carbon.

Abstract

In order to ascertain the suitability of glassy carbon as a material for encapsulation of nuclear waste, glassy carbon was implanted with Xe and the structural changes and surface modification were investigated before and after annealing. This was performed using Raman spectroscopy analysis, high-resolution transmission electron microscopy (HRTEM) measurements, scanning electron microscopy (SEM), and atomic force microscopy (AFM). The Raman spectrum of the implanted sample showed that ion bombardment amorphised the glassy carbon structure. The HRTEM analysis of the virgin glassy carbon exhibited some features which are similar to those of fullerenes. One of the features is the appearance of closed onion-like nanoparticles and several graphitic fringes of varying sizes and orientations embedded in the glassy carbon structure. The presence of the onion-like features, as well as the graphitic fringes within the glassy carbon structure, suggest that glassy carbon is a disordered form of carbon. The HRTEM analysis of the as-implanted sample also shows some dark spots within the implanted region which are likely xenon bubbles. The SEM and AFM analysis showed that the grain size becomes larger and more prominent with increasing annealing temperature, leading to an increase in the surface roughness of glassy carbon.

Keywords: Glassy carbon; HRTEM; Ion implantation; Raman spectroscopy; Structural changes

1. Introduction

Nuclear energy, supplies about 17% of the total electrical energy generated in the world. Further expansion of nuclear energy offers a tempting alternative to relieve and reduce CO_2 emissions to the environment. However, the generation of nuclear energy raises several concerns regarding environmental contamination during the storage of radioactive nuclear waste [1]. This type of nuclear waste should be stored in a segregated method so that it can be retrieved for further treatment, transferred to another storage facility or for disposal [2]. Dry cask storage is a preferred method for storing nuclear waste. The casks are usually made of different materials such as copper, iron, stainless steel, titanium alloys, and nickel-based alloys [3]. These materials are susceptible to degradation due to ageing which can lead to leakage of radioactive material into the environment. Therefore, dry casks with longer lifespan are necessary for nuclear waste. Glassy carbon is an interesting carbon-based material which can be used as an alternative material for dry cask long term storage.

In many reactor designs, the nuclear fuel becomes critical within the graphite core, and during the operation of these reactors, fission products such as Kr, Cs, Cd, Ag, Pd, Xe, etc. are trapped within the structure of the graphite core. Although graphite is a suitable reactor core structural material because of its excellent properties such as low neutron absorption cross section, high resistance to radiation, high heat resistance (sublimation temperature up to 3000 °C) [4], and high thermal conductivity. However, there are several problems associated with graphite reactor core such as irradiation-induced crack propagation and stress from extreme heat fluctuation which can lead to a significant loss of structural integrity in the graphite reactor core over the lifetime of the nuclear reactor. During reactor operation, many of the graphite component physical properties are significantly changed by irradiation. These changes lead to the generation of significant internal contraction stress and thermal shut down stress which could lead to component failure. In addition, if graphite is irradiated to a very high fluence, there can be a rapid reduction in strength, making the component brittle and susceptible to degradation. The problems with the graphite reactor core can be addressed by proposing glassy carbon as a protective layer on graphite.

Glassy carbon is a relatively new allotrope of carbon with very interesting properties different from most other allotropes of carbon. It is a synthetic allotrope of carbon with exceptional properties such as high hardness and strength, impermeability to gases, high-temperature resistance, and high resistance to attack by all chemical acids. Based on these properties, glassy

carbon is a good material for the nuclear industry and related applications [5]. The main advantage of glassy carbon is its stability when exposed to high irradiation fluences.

The structure of glassy carbon has been of major interest to researchers, and several structural models have been proposed since it was first fabricated in the 1960s. The most popular among these models are those by Noda and Inagaki [6] and Jenkins and Kawamura [7]. The model by Noda and Inagaki [6] suggested that glassy carbon consists of a three-dimensional structure consisting of a network of trigonal arrangements of carbon atoms. According to Jenkins and Kawamura [7], the glassy carbon structure contains ribbon-like graphitic domains of sp^2-hybridized carbon atoms. However, the most recent studies using the HRTEM have suggested that glassy carbon has a fullerene-related structure [8, 9] and that the glassy carbon structure changes to that of amorphous carbon after high fluence ion irradiation. Energetic xenon ions are produced via nuclear reactions in high-level waste. Some xenon ions can be implanted in glassy carbon nuclear waste containers.

The structural evolution of glassy carbon caused by Xe ions of 320 keV up to different fluences at RT was investigated [10] and recently the migration of Xe of 200 keV implanted into glassy carbon at room temperature followed by annealing from 600 up to 1500 ^{o}C was investigated by Ismail et al. [11]. In this study, the quantitative Raman analysis of results from [11] are compared with HRTEM analysis of the samples annealed between 600 and 1500 ^{o}C to get more insight into the annealing of defects in Xe implanted glassy carbon. The current study aims to obtain more information on the role of defects/radiation damage caused by xenon ions bombardment in glassy carbon and its effect on the microstructure and surface structure of glassy carbon. Both of these can influence the effectiveness of glassy carbon's ability to contain xenon.

2. Experimental method

Commercially available Sigradur® G glassy carbon substrates were used in this study. Glassy carbon substrates were implanted with 200 keV xenon ions at room temperature to a fluence of 1×10^{16} ions/cm^2. The implantation was performed using the 400 kV ion implanter ROMEO at the Institut für Festkörperphysik, Friedrich-Schiller-Universität, Jena, Germany. The beam current was kept at about 8000 nA while the time was 1 h 3 min along the implantation process, to avoid annealing out of some of the damages due to an increase in the substrate temperature. During implantation, the substrate reached a maximum temperature of about 55 °C. After

implantation, the samples were cut into 10 mm ×5 mm using a tungsten carbide (WC) cutter to ensure that the samples fit into sample holders. The implanted samples were isochronally annealed in vacuum using a quartz tube furnace at temperatures ranging from 600 °C to 1500 °C for 5 h. Fig. 1 shows the as-implanted Xe depth profile obtained from Rutherford backscattering spectrometry (RBS).

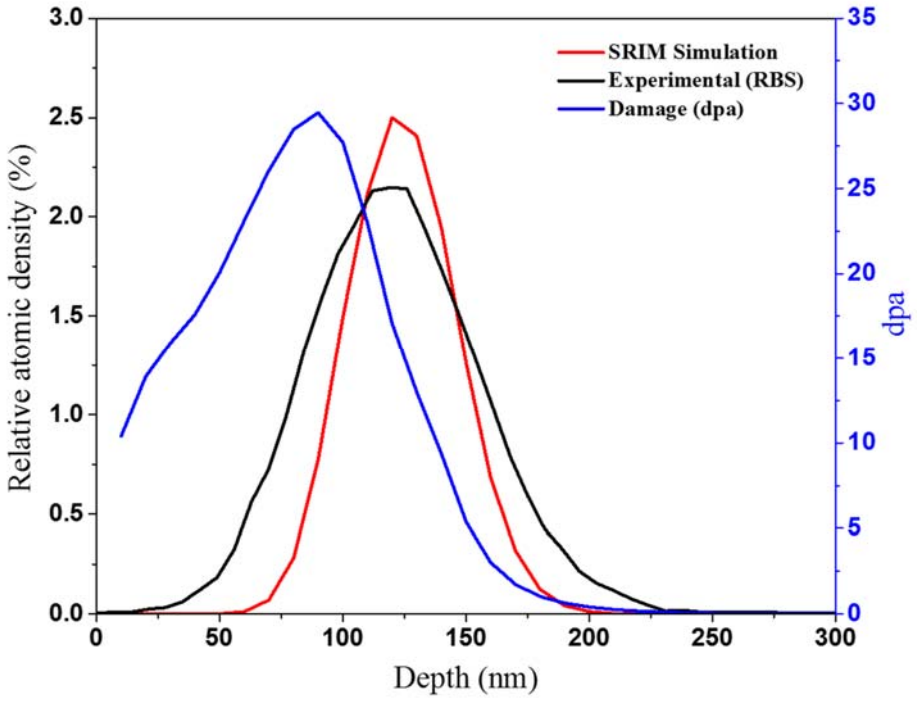

Fig.1: SRIM simulations of the Xe-profile, Xe-profile determined by RBS and SRIM simulation of the damage profile. Taken from Ref [11].

The radiation damage induced by the Xe ions implantation and the effect of heat treatment on the microstructure of the implanted glassy carbon was investigated by the WITec alpha 300 confocal Raman spectroscopy instrument. The 100× /0.9NA objective lens was used to acquire the Raman spectra at the wavelength of 532 nm and laser excitation power of 5 mW.

The glassy carbon surface morphology was investigated by atomic force microscopy (AFM) using the Dimension Icon AFM system in contact mode. The AFM images were recorded at a scale of 1 × 1 μm^2. The root mean square (rms) roughness data were obtained by analyzing the AFM images using the NanoScope Analysis offline software. The AFM results were complemented by scanning electron microscopy (SEM) analysis using the Zeiss Ultra 55 field emission gun scanning electron microscope (FEG-SEM) with an in-lens detector. A 2 kV

accelerating voltage was employed during all SEM imaging. The working distance was maintained at approximately 2.8 mm for all the imaging experiments and different magnifications were used.

The samples for the high-resolution transmission electron microscopy (HRTEM) analysis were prepared using a Ga-ion beam focused ion beam (FIB) technique. A thin platinum protective layer was deposited on the surface of the glassy carbon to avoid any interaction between the FIB beam and the samples. The HRTEM micrographs were obtained in bright field mode, while the low-resolution images were obtained in dark field mode. One of the main differences between the bright field and dark field mode is that different electron populations are used to construct the HRTEM micrograph. In the bright field image, the unscattered (transmitted) electron beam are selected, and the scattered electrons are blocked [12]. Since the unscattered beam is selected, areas with crystalline or high mass materials will appear dark.

3. Results and discussion

When the energetic ions penetrate a solid target, the ions decelerate by transferring their energy to the target atoms via elastic collisions (nuclear stopping) and inelastic collisions (electronic stopping) depending on the ion's energy. During this process, the target atoms can be displaced from their lattice positions to other sites, such as interstitials in the near-surface region, causing deterioration or damage to the microstructure.

In this study, the surface defects in the glassy carbon substrate caused by the implantation of Xe ions at 200 keV were evaluated. Fig. 1 shows the damage accumulated/damage profile in the glassy carbon surface layer in terms of displacement per atom (dpa), calculated from the SRIM simulation compared to the as-implanted Xe depth profile obtained experimentally by RBS analysis. The SRIM simulation was performed in the “Full cascade” mode using the density of 1.42 g/cm^3 for glassy carbon. A threshold energy for carbon atoms displacement of 25 eV was used in the simulation [13]. The maximum level of damage (29 dpa) is much larger than the critical value required for the amorphisation of glassy carbon (0.2 dpa) [10]. Fig. 1 also shows that the maximum damage is at about 90 nm, which is closer to the surface compared to the experimental and simulated Xe depth profiles. The value of 90 nm indicated that a large number of atoms were displaced near the surface of the glassy carbon. Previous studies have shown that at a damage level above 4 dpa, the near-surface region of glassy carbon structure would be completely amorphised [5, 10, 11].

Raman spectroscopy is a non-destructive technique that can be used for structural characterization of carbon-based materials [14, 15]. It was used in this study to monitor the microstructural changes induced in the glassy carbon by bombardment and thereafter, thermal annealing. Although, depending on the laser excitation power, Raman spectroscopy is generally non-destructive. However, damage or annealing of the sample can occur at high laser excitation power. Only qualitative analysis was reported in the previous paper [11] which mainly focused migration of Xe in glassy carbon. In this study, we focus on the quantitative structural analysis of Raman results.

The microstructure of the virgin glassy carbon after Xe ions implantation, and annealing at high temperatures was investigated. The results are shown in Fig. 2 (a-c). Fig. 2 (a) shows the Raman spectrum obtained from the virgin glassy carbon whose the main features are the *D* and *G* peaks, which lie at around 1346 cm^{-1} (*D*-peak) and 1591 cm^{-1} (G-peak) for a 532 nm excitation laser. The D peak originates from a disorder usually present in the structure of the graphitic amorphous materials such as glassy carbon and fullerenes. However, the G peak is attributed to the in-plane stretching vibrational mode of the sp^2 bonds [16]. The Raman spectrum of the virgin glassy carbon also has an extra peak (D'-peak), which usually exists in graphitic amorphous carbon materials with a very small size of the sp^2 domains that exist in glassy carbon thereby displaying (*G* + *D′*) Raman doublet [17].

To analyse the Raman spectrum obtained from the virgin glassy carbon and after annealing at temperatures (600 –1000 °C) in steps of 100 °C and 1500 °C for 5 h, a combination of Lorentzian and Breit-Wigner-Fano (BWF) functions was used to fit the D and G peaks. For the as-implanted spectrum, only the BWF fit was used since the Lorentzian-BWF combination could not be employed due to the merging of the D and G peaks into a single broad band which could no longer be distinguished.

The I_D/I_G intensity ratio of the D and G peaks of the virgin glassy carbon was found to be 1.63. Using the Tuinstra-Koenig equation ($La = C(\lambda)/(I_D/I_G)$), where $C(\lambda)$ is the laser wavelength-dependent constant, $C(\lambda) = 4.96$ nm for $\lambda = 532$ nm, [18]. The in-plane average crystallite size, L_a was calculated to be 3.04 nm. However, the Tuinstra-Koenig equation is only valid for crystallite sizes of between $2.5 < L_a < 300$ nm [10].

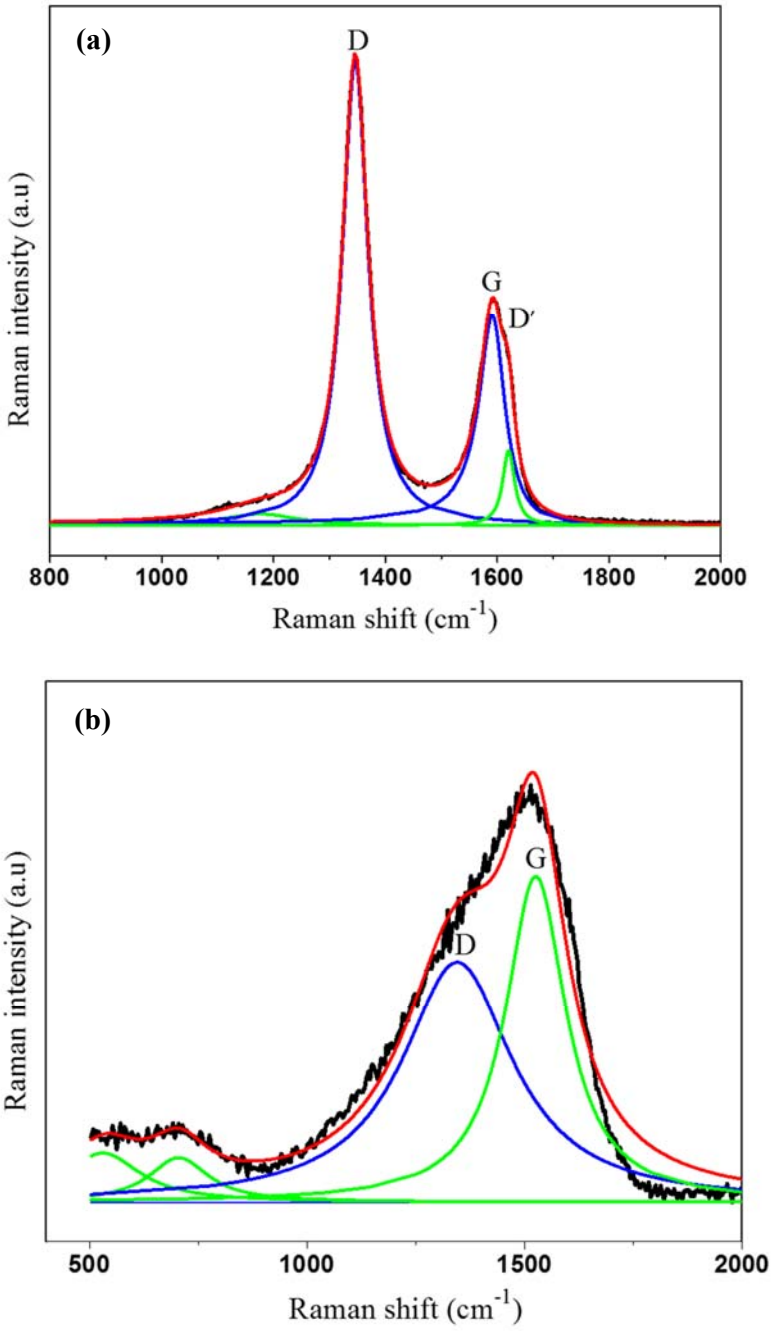
(a)
D
G
D′
Raman intensity (a.u)
800
1000
1200
1400
1600
1800
2000
Raman shift (cm-1)
(b)
G
D
Raman intensity (a.u)
500
1000
1500
2000
Raman shift (cm-1)

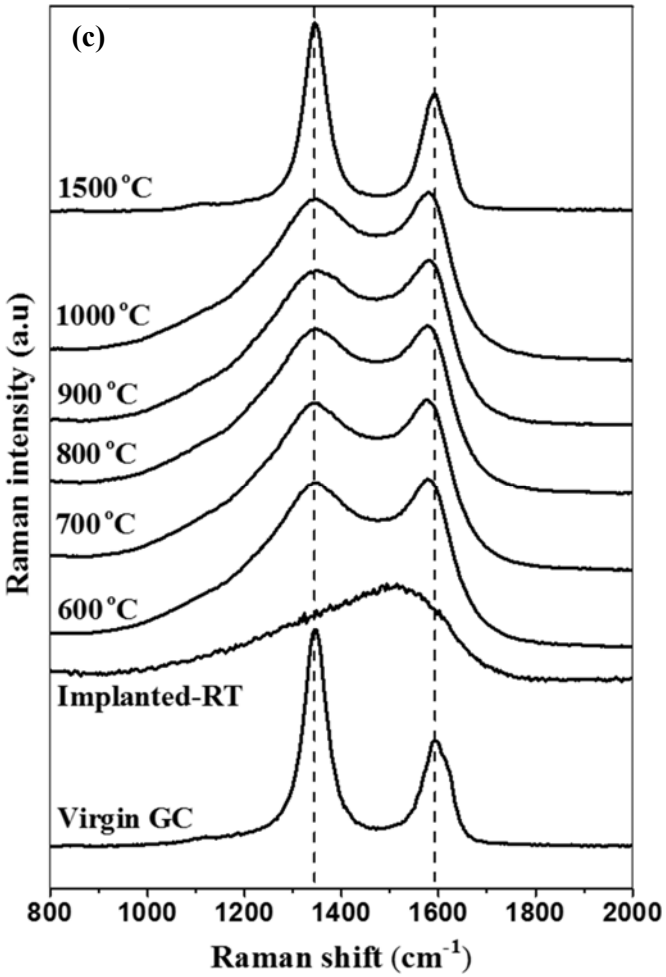

Fig. 2: Raman spectra of (a) virgin glassy carbon (b) after the 200 keV Xe ions implantation at room temperature (c) after annealing at temperatures from 600 °C to 1000 °C and 1500 °C.

The Raman spectrum of the Xe implanted glassy carbon is shown in Fig. 2 (b). In the current study, the deconvolution of the Raman spectrum after Xe ions implantation showed that the G peak shifted to 1528 cm^{-1} after implantation. This shift to the lower wavenumber is due to the damage in the nano-crystalline structure that occurred within the implanted region. This was expected since the dpa level of 200 keV Xe implantation was higher than the threshold value required to damage the glassy carbon structure of 0.2 dpa. This observation was confirmed by the HRTEM results discussed later in this article.

The I_D/I_G ratio significantly reduced from the virgin glassy carbon value of 1.63 to 0.74 after implantation, which indicated the reduction in the average crystallite size. Since the Tuinstra-Koenig relation is no longer valid for the smaller crystallite size, the Ferrari et al. [17] equation

was used. A value of 1.16 nm was obtained and this confirmed that the high fluence implantation had damaged the glassy carbon structure and reduced the crystallite size.

The Raman spectra of the implanted glassy carbon samples annealed from 600 to 1000 °C and at 1500 °C are shown in Fig. 2 (c). Annealing from 600 to 1000 °C showed that the D and G peaks became more apparent which indicated a slight recovery in the glassy carbon structure. Generally, the recovery of the glassy carbon structure is expressed by the reappearance of the D and G peaks. No noticeable shift in the D peak position was observed after annealing from 600 to 1000 ° C while the G peak position shifted to higher wavenumbers (located at 1581 cm^{-1} after annealing at 1000 °C). After fitting the D and G peaks of Raman spectra of the samples annealed from 600 to 1000 °C, the average crystallite size was found to be 1.30 ± 0.02 nm. After annealing the implanted sample at 1500 °C, the D peak position remained unchanged while the G peak position shifted to 1593 cm^{-1}. The G peak position after annealing at 1500 °C was 2 cm^{-1} higher than that of virgin glassy carbon. This may suggest the presence of the compressive stress in the carbon bonds due to a change in inter-atomic distances. The average crystallite size after annealing at this temperature was found to be 3.12 nm which is comparable to that of the virgin glassy carbon (3.04 nm). After annealing at 1500 °C, the D and G peaks became more distinguishable and located close to the virgin glassy carbon peak positions indicating a highly recovered glassy carbon structure.

The effect of excitation laser power on the Raman spectra was analysed by comparing the spectra obtained in this study at 5 mW and wavelength of 532 nm to those obtained at an excitation power of 1 mW and wavelength of 514.5 nm [11]. Neither new spectral bands emerged nor were the existing bands lost, indicating that no major structural changes caused by the higher excitation laser power.

For the wavelength of 532 nm (this study), the effective penetration depth was found to be around 59 nm using equation $z = \frac{\lambda}{4\pi k}$ [11]. In our case, the projected range (R_p) of the as-implanted Xe depth profile is about 119.3 nm and the range straggling of ΔR_p is 34.2 nm as predicted by SRIM simulation which indicates an amorphous layer (the thickness of the implanted area, $R_p + 3\Delta R_p$) approximately 222 nm thick from the surface. Therefore, only the Xe implanted region of the glassy carbon substrate was analysed.

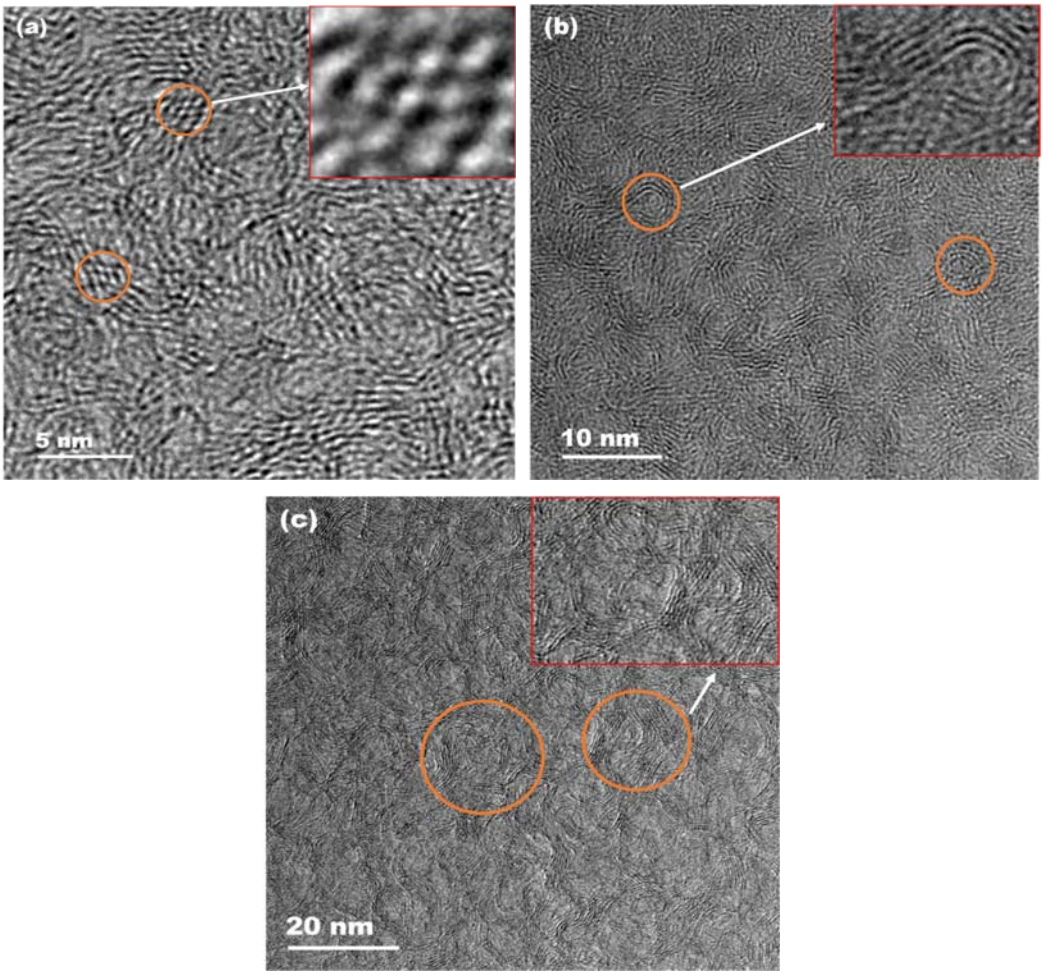

Fig. 3: The HRTEM micrographs of the virgin glassy carbon obtained at different magnifications. The graphitic fringes with different sizes and orientations are highlighted in the brown circles in Fig. (a). The onion-like structures of glassy carbon are highlighted in the brown circles in Figs. (b) and (c).

The high-resolution transmission electron microscopy (HRTEM) has been extensively and successfully used to analyse crystal structures and crystal lattice imperfections in various materials at an atomic scale. Fig. 3 shows the bright field cross-sectional HRTEM micrographs of the virgin glassy carbon. In Fig. 3 (a) several graphitic fringes of varying sizes and orientations embedded within the glassy carbon structure can be observed. Other features observed in glassy carbon are the closed onion-like nanoparticles within the structure which are highlighted by circles in Fig. 3 (b). Fig. 3 (c) shows the onion-like features accompanied by closed fullerene type of nanostructures. These can be compared to the imperfect multilayer fullerene that often surrounds pores. Previous HRTEM studies of glassy carbon have shown that it exhibits some features which are similar to that of fullerenes [19, 20]. However, all these

structures observed do not have long-range graphitic ordering and there is disorder in structure. This is responsible for the G peak (graphitic) and D peak (disorder) observed in Raman spectroscopy analysis. The presence of the onion-like features, as well as the graphitic fringes within the glassy carbon structure, suggests that glassy carbon is a disordered form of carbon. These structural observations in virgin glassy carbon make it different from other forms of non-graphitising carbon and account for its low reactivity and its high impermeability to gases.

Fig. 4 shows the bright field cross-sectional HRTEM micrographs of Xe implanted glassy carbon. Three distinct regions can be observed in Fig. 4 (a). The region (i) is the platinum protective layer, (ii) is the Xe implanted layer, and (iii) the bulk of glassy carbon. In the bulk region several sharply contrasting areas can be seen. The dark spots indicate regions where the electron beam is diffracted, thereby indicating the presence of nano-crystallites. The implanted layer has a thickness of approximately 180 nm which is slightly less than the 222 nm obtained from the RBS spectrum. Studies have shown that the density of glassy carbon increases after ion implantation [10].

Fig. 4 (b) shows some dark spots within the implanted layer which are likely xenon bubbles formed in the implanted region. Xenon is known to form bubbles in several materials including glassy carbon [21, 22]. The presence of dark spots within the implanted layer also suggests that the implanted region was not 100 % amorphous but still contains some graphitic structures. The figure also shows the disappearance of the onion-like features that were present in the virgin glassy carbon as seen in Fig 3. There are few smaller graphitic fringes of different orientations (shown by the red arrows in Fig. 4 (b)) indicating that the glassy carbon structure was damaged after implantation. The structure of glassy carbon within the implanted layer is very similar to that of some amorphous forms of carbon such as soot [23]. The above results are in complete agreement with the Raman spectroscopy results shown in Fig. 2 where the Xe implantation was seen to have damaged the glassy carbon structure.

McCulloch et al. [10] also studied the formation of preferred orientation in glassy carbon due to high fluence Xe^+ implantation. They found out that the implantation of 5×10^{16} Xe^+/cm^2 resulted in the amorphisation of the implanted region. They also observed several graphitic fringes embedded within the amorphised region which had a spacing of approximately 0.34 nm which corresponds to the (002) lattice spacing of graphite.

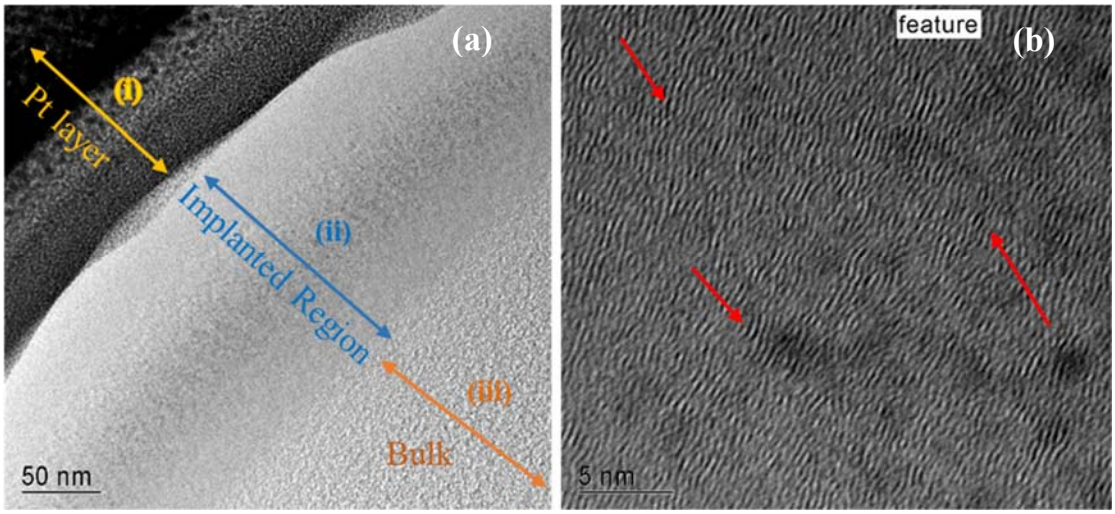

Fig. 4: The HRTEM micrographs obtained at different magnifications showing the effect of the Xe ion bombardment on glassy carbon (a) (i) the contrast between the Pt protective layer (ii) the implanted layer (iii) the bulk of the glassy carbon (b) the Xe implanted glassy carbon at a higher magnification. The red arrows in the image show some of the graphitic fringes present after ion bombardment.

The bright field HRTEM micrographs obtained at different magnification after annealing at 600 °C are shown in Fig. 5. Fig. 5 (a) also depicts the contrast between the Pt layer, the implanted region, and the bulk of the glassy carbon sample. A key observation is the disappearance of the Xe bubbles that were observed in Fig. 4 (a). This indicates that the Xe bubbles formation only took place during the implantation process. As the annealing temperature increases, the onion-like carbon structures become more dominant [19]. Another observation from Fig. 5 (b) is the appearance of some intertwined nano-structures (highlighted with red circles) that were absent in the as-implanted HRTEM images. The presence of these nano-structures suggests that after annealing at 600 °C, partial recovery of the glassy carbon structure had started to occur.

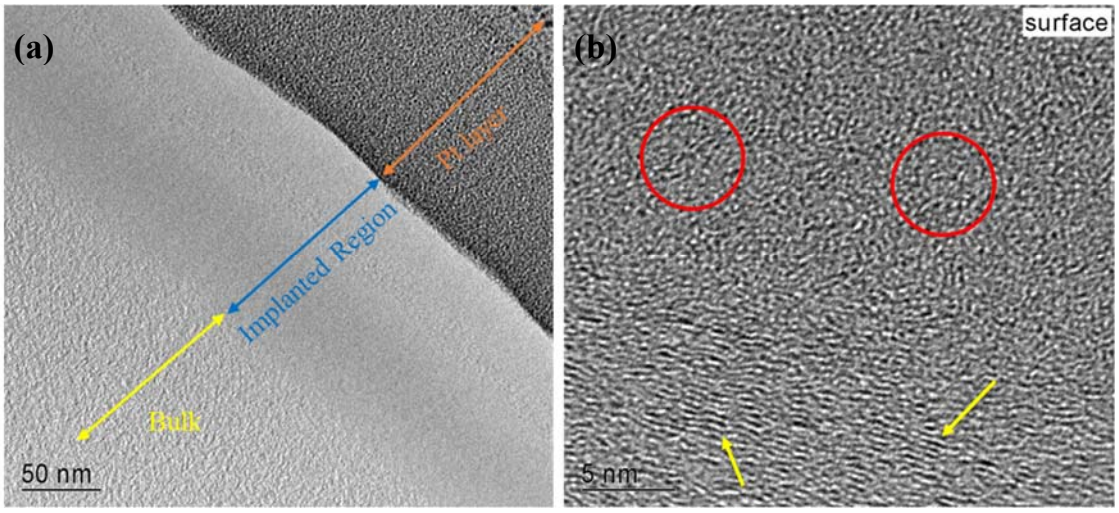

Fig. 5: The bright field of the HRTEM images obtained at different magnification after annealing at 600 °C (a) the contrast between the Pt layer, the implanted layer, and the bulk of the glassy carbon (b) intertwined nano-structures (red circles) and graphitic fringes (yellow arrows).

Fig. 6 shows the HRTEM micrograph of the Xe implanted glassy carbon sample annealed at 1000 °C for 5 h. A clear distinction between the HRTEM micrograph of the sample annealed at 600 °C and that annealed at 1000 °C can be observed. One key feature is the reduction of the graphitic fringes compared to the as-implanted and the 600 °C annealed samples. The graphitic fringes have been replaced with several intertwined nano-structures (some of them are highlighted with red circles in Fig. 6). The presence of these nano-structures suggests that annealing at 1000 °C resulted in the further recovery of the structure of glassy carbon. However, it is evident that after annealing at 1000 °C, the glassy carbon microstructure did not fully recover to that of virgin glassy carbon. This observation correlates the Raman spectroscopy results of implanted glassy carbon annealed at 1000 °C where the D and G peaks were not similar to the virgin glassy carbon.

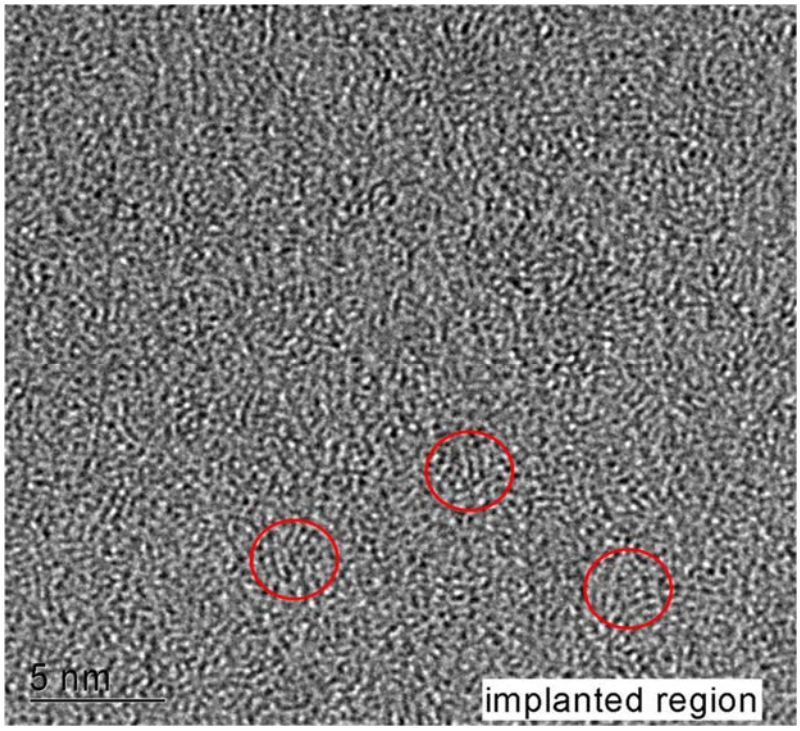

Fig. 6: HRTEM micrograph showing the effect of 1000 °C on the microstructure of the glassy carbon.

To investigate the effect of xenon ions bombardment on the surface roughness and morphology evolution of the glassy carbon, SEM analysis complemented by the AFM analysis were performed. The AFM analysis was done to characterize the surface roughness of the glassy carbon before (Fig. 7 (a)) and after (Fig. 7 (b)) ion bombardment. Different measurements were taken on different surface regions to obtain the R_{rms} (root mean square roughness). The 2D (height and deflection images) and 3D AFM images were obtained using NanoScope Analysis software. Consequently, the two deflection images in Fig. 7 only show features where the normal AFM images had high deviations.

The R_{rms} value obtained for the virgin glassy carbon sample from Fig. 7 (a) is 1.71 nm indicating that the surface was relatively smooth. After the Xe ion bombardment, the R_{rms} value increased to 2.54 nm (see Fig. 7 (b)). The SEM images (see Fig. 8) show that the polishing marks became more visible after the xenon ion bombardment. This can be due to the enhanced sputtering rate of the carbon atoms in the vicinity of the polishing marks. This is attributed to the binding energies of those surface atoms being lower leading to enhanced sputtering.

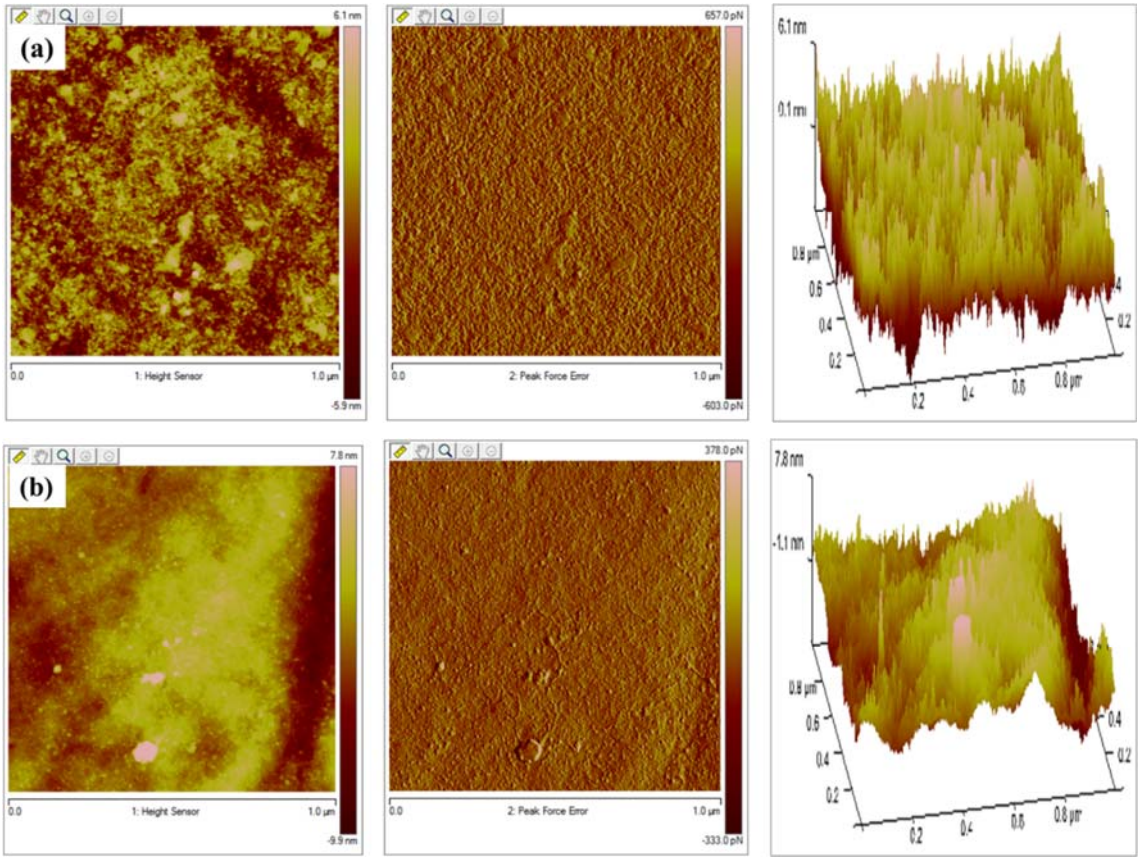

Fig. 7: The AFM (height, deflection error, and 3D) micrographs for (a) the virgin glassy carbon (b) after xenon ion implantation.

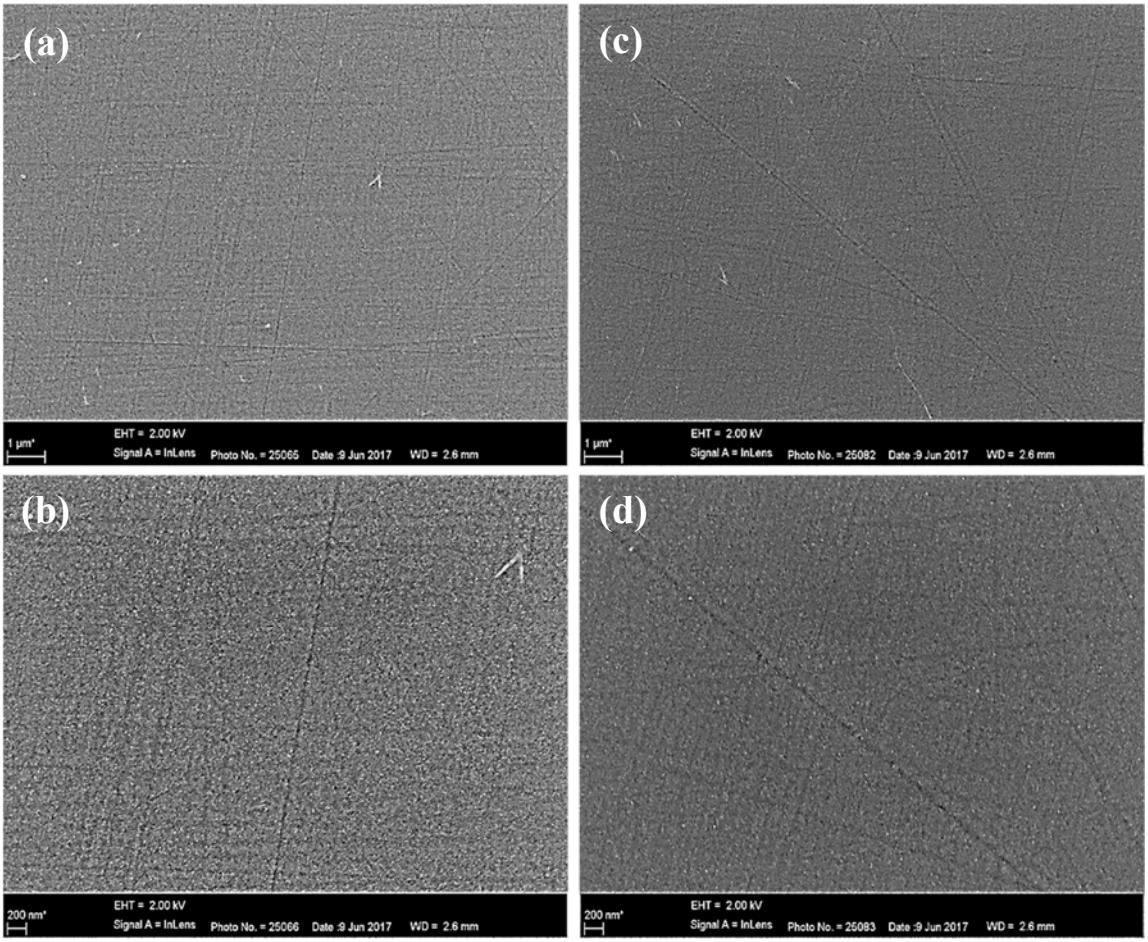

Fig. 8: SEM micrographs obtained at different magnifications, (a-b) virgin glassy carbon (c-d) after xenon ion bombardment.

Fig. 9 (a-b) shows the AFM images obtained after annealing at 1000 °C and 1500 °C. No considerable change in the surface roughness after annealing from 600 °C to 900 °C was observed (not shown here). The R_{rms} value of 1.36 nm was obtained after annealing at a temperature of 1000 °C, indicating a significant decrease in surface roughness (Fig. 9 (a)). The smoothening of the glassy carbon surface at this temperature is attributed to the surface diffusion of the substrate atoms from the sputter roughened peak to the valley positions [24, 12]. After annealing at 1500 °C (Fig. 9 (b)) the grain size becomes larger and more prominent. Embedded on the surface are several sharpened columnar structures with varying heights increasing the glassy carbon's surface roughness. The brighter spots shown in the 2D AFM image (Fig. 9 (b)) indicate the top of the columnar structures and the dark spots indicate the valleys. Increase in annealing temperature caused the increase in grain size as seen in Fig. 10 (higher magnification SEM image). These results are well agreement with the AFM results for

a sample annealed at 1500 °C shown in Fig. 9 (b). This phenomenon can be attributed to the coalescing or accumulation of the surface clusters into the large grain with increasing temperature.

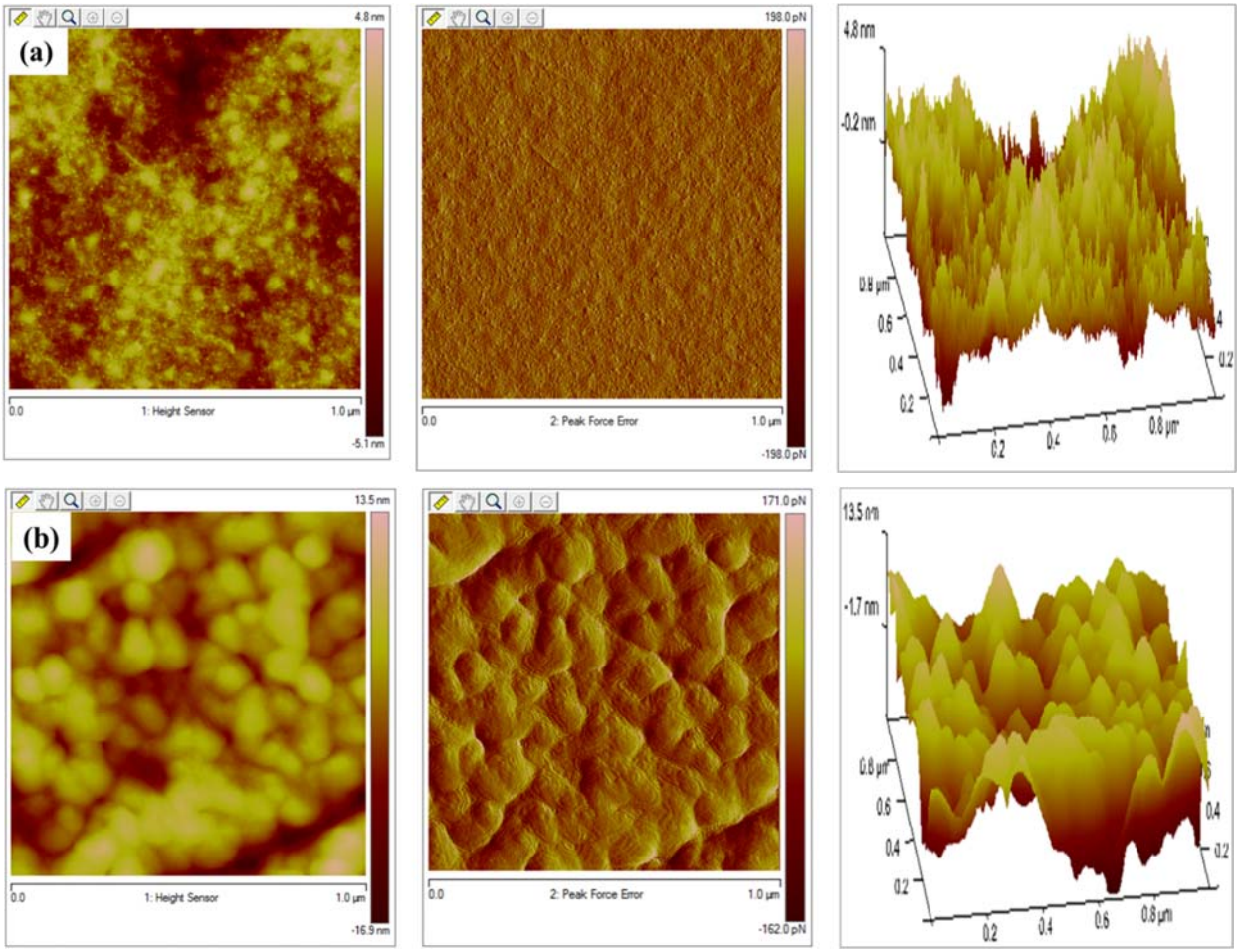

Fig. 9: AFM (height, deflection error, 3D height) images of samples annealed at (a) 1000 °C and (b) 1500 °C.

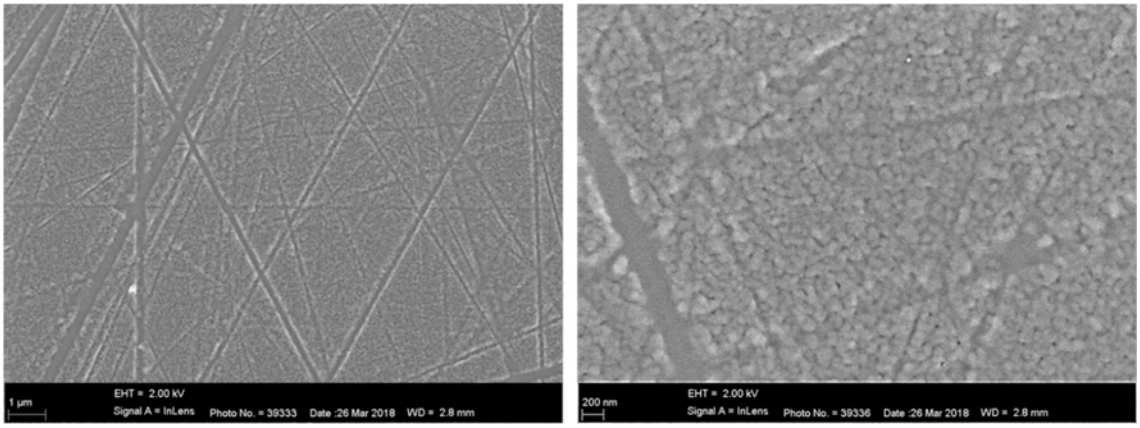

Fig. 10: SEM micrographs of Xe implanted in glassy carbon and annealed at 1500 °C for 5h. The images were obtained at different magnifications.

4. Conclusion

The effect of xenon ions implantation and vacuum annealing on the structural changes and surface modification of the glassy carbon was investigated. The Raman spectrum obtained after the Xe implantation resulted in the D and G peaks merging into single broadband which indicated amorphisation in the damaged region. Annealing at temperatures ranging from 600 °C to 1000 °C for 5 h showed only partial recovery in the glassy carbon structure accompanied by an increased average crystallite size as determined by the (I_D/I_G) intensity ratio. The significant recovery of the glassy carbon microstructure was observed after annealing at a temperature of 1500 °C which has an average crystallite size of 3.12 nm. The HRTEM analysis of the as-implanted sample showed some dark spots within the implanted layer which are likely xenon bubbles formed in the implanted region. The as-implanted sample also showed a few very small graphitic fringes of different orientations confirming that the glassy carbon structure was damaged after implantation. The AFM and SEM results indicated the surface roughness increased after Xe^+ implantation and increased with increasing annealing temperature generally, accompanied by grain growth.

Acknowledgement

Financial support by the COMSATS University Islamabad (CUI) and The World Academy of Sciences (TWAS) is gratefully acknowledged.

References

[1] F. L. Toth, H. H. Rogner, Oil and nuclear power: Past, present, and future, Energy Econ. **28** (2006) 1 – 25.

[2] IAEA, safety standards: Storage of radioactive waste, Vienna, 2006.

[3] M. Yim, K.L. Murty, Materials issues in nuclear-waste management, J.Min. Met. & Mat. Soci. **52** (2000) 26 – 29.

[4] T. Takeda, Y. Inagaki, High Temperature Gas-cooled Reactors, Elsevier Inc., 2021.

[5] E.G. Njoroge, T.T. Hlatshwayo, M. Mlambo, O. Odutemowo, K.A. Annan, V. A. Skuratov, M. Ismail, J.B. Malherbe, Effect of thermal annealing on SHI irradiated indium implanted glassy carbon, Nucl. Instru. Meth. Phy. Res. **B 502** (2021) 66 – 72.

[6] T. Noda, M. Inagaki, The structure of glassy carbon, Bull. Chem. Soci. Jap. **37** (1964) 1534 – 538.

[7] G. M. Jenkins, K. Kawamura, Structure of glassy carbon, Nature **231** (1971) 175 – 176.

[8] P. J. F. Harris, Structure of non-graphitising carbons, Int. Mat. Rev. **42** (1997) 206 – 218.

[9] P. J.F. Harris, New perspectives on the structure of graphitic carbons, Criti. Rev. Sol. Sta. Mat. Sci. **30** (2005) 235 – 253.

[10] D.G. McCulloch, S. Prawer, A. Hoffman, Structural investigation of xenon-ion-beam-irradiated glassy carbon, Phy. Rev. B **50** (1994) 5905 – 5917.

[11] M.Y.A. Ismail, Z.A.Y. Abdalla, E.G. Njoroge, O.S. Odutemowo, T.T. Hlatshwayo, E. Wendler, V.A. Skuratov, J.B. Malherbe, Effect of high temperature annealing and SHI irradiation on the migration behaviour of Xe implanted into glassy carbon, Nucl. Instru. Meth. Phy. Res. **B 489** (2021) 11–19.

[12] Introduction to Materials Characterization: https://chem.libretexts.org. (Accessed November 25, 2020).

[13] J. F. Ziegler, SRIM-2013, http://www.srim.org. (Accessed July 19, 2019).

[14] A.C. Ferrari, J. Robertson, Determination of bonding in diamond-like carbon by Raman spectroscopy, Diam. Rel. Mat. **11** (2002) 1053 – 1061.

[15] S. Prawer, F. Ninio, I. Blanchonette, Raman spectroscopic investigation of ion-

beam irradiated glassy carbon, J. Appl. Phys. **68** (1990) 2361 – 2366.

[16] Meng Hu, Shuangshuang Zhang, Bing Liu, Yingju Wu, Kun Luo, Zihe Li, Mengdong Ma, Dongli Yu, Lingyu Liu, Yufei Gao, Zhisheng Zhao, Yoshio Kono, Ligang Bai, Guoyin Shen, Wentao Hu, Yang Zhang, Ralf Riedel, Bo Xu, Julong H, Yongjun Tian, Heat-treated glassy carbon under pressure exhibiting superior hardness, strength and elasticity, J. Materiomics **7** (2021) 177–184.

[17] A.C. Ferrari, J. Robertson, Interpretation of Raman spectra of disordered and amorphous carbon, Phys. Rev. B **61** (2000) 14095 – 14107.

[18] M. J. Madito, M. Y. A. Ismail, T. T. Hlatshwayo, C. B. Mtshali, The nature of surface defects in Xe ion implanted glassy carbon annealed at high temperatures: Raman spectroscopy analysis, Appl. Surf. Scie. 506 (2020) 145001.

[19] K. Jurkiewicz, M. Pawlyta, D. Zygadło, D. Chrobak, S. Duber, R. Wrzalik, A. Ratuszna, and A. Burian, Evolution of glassy carbon under heat treatment: correlation structure-mechanical properties, J. Mat. Sci. **53** (2018) 3509 – 3523.

[20] P. J. F. Harris, Fullerene-related structure of commercial glassy carbons, Philo. Mag. **84** (2004) 3159 – 3167.

[21] D. McCulloch, S. Prawer, Bubbles in xenon implanted glassy carbon, J. Comput. Assist. Microsc. **4** (1992) 281 – 285.

[22] D. McCulloch, S. Prawer, A. Hoffman, D. K. Sood, Cross-sectionals transmission electron microscopy investigation of xenon irradiated glassy carbon, Nucl. Instru. Meth. Phy. Res. **B 80/81** (1993) 1480 – 1484.

[23] H. A. Calderon, A. Okonkwo, I. Estrada-Guel, V. G. Hadjiev, F. Alvarez-Ramírez, F. C. Robles Hernández, HRTEM low dose: the unfold of the morphed graphene, from amorphous carbon to morphed graphenes, Advanced Stru. Chem. Imag. **2:10** (2016) 1 – 12.

[24] J.B. Malherbe, Bombardment-induced ripple topography on GaAs and InP, Nucl. Instrum. Methods Phys. Res. B212 (2003) 258 - 263